Australian Government
Department of Defence
Defence Science and
Technology Organisation

Coherent Multilook Radar Detection for Targets in Pareto Distributed Clutter

Graham V. Weinberg

Electronic Warfare and Radar Division

Defence Science and Technology Organisation

DSTO–TR–2646

ABSTRACT

The Pareto distribution has been proposed recently as a model for intensity clutter measurements, for maritime high resolution radar returns. Using the theory of spherically invariant random processes, the Neyman-Pearson optimal detector is derived. The generalised likelihood ratio test yields a simple sub-optimal approximation, and its performance is gauged against the whitening matched filter.

APPROVED FOR PUBLIC RELEASE

APPROVED FOR PUBLIC RELEASE

Coherent Multilook Radar Detection for Targets in Pareto Distributed Clutter

Executive Summary

This work supports the Microwave Radar Branch's research efforts in the area of high grazing angle detection of small maritime targets from an airborne surveillance platform. It contributes to the research requirements of Task 07/040 (Support to AIR 7000[1]). Detection of targets is a major function of radar systems, and hence detector performance is an important component in the efforts of Task 07/040. Detectors are designed to find targets within specific clutter models. Recently it was found the simple Pareto Distribution fitted high grazing angle clutter quite well. This was validated using the DSTO Ingara data, collected in a trial during 2004. Hence it is necessary to investigate the design of radar detection schemes in such a clutter environment.

The theory of spherically invariant random processes (SIRPs) puts this problem into a formulation that allows the determination of detection decision rules. The Pareto distribution is put into this framework, and the Neyman-Pearson detector is specified. Due to intractibility of the latter, several suboptimal approximations are considered. The major contribution of this work is to examine coherent multilook detection under the assumption of a Pareto clutter model. Although the Pareto SIRP and form of the generalised likelihood ratio test for detection has been presented already in the literature, it has not been applied directly to the multilook problem under consideration.

In addition to this, it will be shown that for Pareto models whose parameters are typical of clutter obtained from a radar operating in vertical polarisation, the whitening matched filter is an appropriate suboptimal detector. This is useful because the generalised likelihood ratio test solution depends on clutter parameters, unlike the whitening matched filter.

---

[1]Future Maritime Patrol and Response Capability.

Author

Graham V. Weinberg

EWRD

G. V. Weinberg works in the Microwave Radar Branch, in the area of radar detection. He studied mathematics at the University of Melbourne during the 1990s.

Contents

Figures

1   Preliminaries

1.1   Introduction

The Pareto distribution [1, 2] is a simple power law model that has been proposed as an alternative to the more complex high resolution radar maritime clutter models such as the K- and KK-Distributions [3]. It has been validated both for the case of low, as well as high, grazing angle sea clutter returns [4, 5]. Its advantage is that it is a much simpler model that only requires two parameters to be fitted, and its performance matches that of other modern clutter models. Given this, it is thus important to investigate detection schemes for targets in Pareto distributed clutter. In order to achieve this it is necessary to construct the multidimensional clutter and signal probability distribution functions (pdfs). Such an exercise is quite challenging and so a general framework is required. The theory of spherically invariant random processes (SIRPs) [6-9] provides a solution to this problem. Such processes model the clutter in the complex domain as a product of a nonnegative random variable S, and a zero mean complex Gaussian process $\mathcal{G}$. The latter process and S are assumed to be independent, and $\mathcal{G}$ has a $N \times N$ covariance matrix Σ. We will assume the latter is semi-positive definite, so that its inverse possesses a Cholesky decomposition, as in [10].

The application of the Pareto distribution to sonar detection performance is outlined in [7], which is a useful reference on the analysis to follow. Here we focus on the radar detection problem, based upon a series of N returns, which differs significantly from the application in [7], although the mathematical derivations of detectors is similar.

Coherent multilook radar detection for targets embedded within Pareto distributed clutter has been introduced in [11], which includes generalised likelihood ratio test detectors and comparison to whitening matched filters. The Pareto distribution is embedded within a spherically invariant random process (SIRP), which enables the decision rules to be determined. The Pareto distribution has been shown in [12] to arise as the intensity distribution of a compound Gaussian model for which a linear threshold detector is optimal. Other recent applications of the Pareto distribution to radar include [13, 14] who use the fact that from extreme value theory, the tail of any distribution can be modelled as

a generalised Pareto distribution. Consequently, CFAR processes are derived for targets in Pareto distributed clutter. However, the resultant threshold/false alarm probability relationship is dependent on both Pareto parameters, which is a significant shortcoming. A Bayesian approach to constructing Pareto CFAR detectors is outlined in [15], but the resultant threshold/false alarm probability relationship is not amenable to numerical methods. Coherent radar detection for the Pareto distribution has also been considered in [16], from the point of view of a compound Gaussian model with inverse gamma texture[1]. It is shown that the CFAR property does not hold in general for coherent detection schemes considered. However, this is addressed by introducing some conditions under which a CFAR process can be produced.

1.2   Structure and Contributions

The report does not present a detailed analysis of SIRPs but instead derives the appropriate properties directly as required. This is also specialised to the problem under consideration, which simplifies the form of the detector by applying a whitening approach first. Section 2 formulates the multilook detection problem. In addition, the Pareto SIRP is introduced. Although this is presented in [7], the main difference is the performance of multilook detection schemes for radar are considered here. The optimal Neyman-Pearson detector is constructed in Section 3 for the case of a completely known target model. This assumption is then relaxed, by constructing the generalised likelihood ratio test (GLRT), as a suboptimal approximation to the optimal detector. Section 4 analyses the performance of the GLRT detector by comparing it with a whitening matched filter approximation. Detector performance is based upon a Gaussian target model, embedded within clutter whose parameters have been estimated from Ingara data sets. This is in contrast to the numerical analysis in [16], whose Pareto parameter values used do not correspond to those estimated from real clutter. As a consequence of this, it will be shown the whitening matched filter can be used as a good suboptimal detector for a number of scenarios.

---

[1]This paper was published at the time this report was first written

2   Detection Problem Structure

2.1   Spherically Invariant Random Processes

Spherically Invariant Random Processes (SIRPs) provide a general formulation of the joint density of a non-Gaussian random process, enabling the construction of densities for Neyman-Pearson detectors [2, 17]. Traditionally, a SIRP is introduced as a process whose finite order subprocesses, called Spherically Invariant Random Vectors (SIRVs), possess a specific density [18, 19]. However, due to an equivalent formulation, we can specify SIRVs and SIRPs in a manner more intuitive to the modelling of radar returns as follows. Let $\boldsymbol{c} = \{c_1, c_2, \ldots, c_N\}$ be the complex envelope of the clutter returns. Then this vector is called SIRV if it can be written in the compound-Gaussian formulation

$$\boldsymbol{c} = S\boldsymbol{\mathcal{G}}, \tag{2.1}$$

where the process $\boldsymbol{\mathcal{G}} = (G_1, G_2, \ldots, G_N)^T$ is a zero mean complex Gaussian random vector, or multidimensional complex Gaussian process, and S is a nonnegative real valued univariate random variable with density f_S. The latter random variable is assumed to be independent of the former process. If such a decomposition exists for every $N \in \mathbb{N}$ the complex stochastic process $\{c_1, c_2, \ldots\}$ is called spherically invariant. For a comprehensive description of the modelling of clutter via SIRPs consult [18]. What is clear from the formulation (2.1) is that, by conditioning on the random variable S, we can write down the density of $\boldsymbol{c}$ as a convolution. This will be shown explicitly in the analysis to follow.

2.2   General Formulation

The detection decision problem is now formulated. We assume that we have a SIRP model for the clutter $\boldsymbol{c}$ as specified through the product formulation (2.1). Suppose the radar return is $\boldsymbol{z}$, which is a complex $N \times 1$ vector. Then the coherent multilook detection problem can be cast in the form

$$H_0 : \boldsymbol{z} = \boldsymbol{c} \text{ against } H_1 : \boldsymbol{z} = R\boldsymbol{p} + \boldsymbol{c}, \tag{2.2}$$

where all complex vectors are $N \times 1$, and H_0 is the null hypothesis (return is just clutter) and H_1 is the alternative hypothesis (return is a mixture of signal and clutter). Statistical

hypothesis testing is outlined in [2]. Here, the vector $\boldsymbol{p}$ is the Doppler steering vector, whose components are given by $\boldsymbol{p}(j) = e^{-j2\pi i f_D}$, for $j \in \{0, 1, \ldots, N-1\}$, where f_D is the normalised target Doppler frequency, and $-0.5 \le f_D \le 0.5$. It will be assumed that this is completely known. The complex random variable R accounts for target characteristics, and $|R|$ is the target amplitude. Suppose the zero mean Gaussian process has a covariance matrix $\mathbf{cov}(\boldsymbol{\mathcal{G}}) = \mathbb{E}(\boldsymbol{\mathcal{G}}\boldsymbol{\mathcal{G}}^H) = \Sigma$. Since it is a covariance matrix, its inverse will exist. It can be shown that the inverse of Σ is symmetric and positive definite. If we assume it is semi-definite positive, then we can apply a whitening filter approach to simplify the detection problem. Hence we suppose the Cholesky Factorisation exists for Σ^{-1}, so that there exists a matrix A such that $\Sigma^{-1} = A^H A$.

A SIRP is unaffected by a linear transformation [6]. This means that applying a linear operator to the clutter process alters the complex Gaussian component, but the characteristic function of the SIRP is preserved. Hence in the literature, a whitening approach is often applied to the detection problem of interest. Note that, by applying the Cholesky factor matrix A to the statistical test, we can reformulate (2.2) in the statistically equivalent form

$$H_0 : \boldsymbol{r} = \boldsymbol{n} \text{ against } H_1 : \boldsymbol{r} = R\boldsymbol{u} + \boldsymbol{n}, \tag{2.3}$$

where $\boldsymbol{r} = A\boldsymbol{z}$, $\boldsymbol{n} = A\boldsymbol{c}$ and $\boldsymbol{u} = A\boldsymbol{p}$.

The transformed clutter process $\boldsymbol{n} = SA\boldsymbol{\mathcal{G}}$, and $A\boldsymbol{\mathcal{G}}$ is still a multidimensional complex Gaussian process, with zero mean but covariance $\mathbf{cov}(A\boldsymbol{\mathcal{G}}) = \mathbb{E}(A\boldsymbol{\mathcal{G}}\boldsymbol{\mathcal{G}}^H A^H) = A\Sigma A^H$.

Since $\Sigma^{-1} = A^H A$, it follows that $I_{N \times N} = \Sigma A^H A$, from which it is not difficult to deduce that $A = (A\Sigma A^H)A$. Let $B = A\Sigma A^H$, then note that $B^2 = B$, so that B is idempotent. Also, it follows that B must be invertible, since $det(B) = det(A)det(\Sigma)det(A^H)$ and $det(\Sigma) \ne 0$ and $det(\Sigma^{-1}) = det(A^H)det(A) \ne 0$. Thus it follows that B must be the $N \times N$ identity matrix. Consequently, we conclude that the transformed Gaussian process $A\boldsymbol{\mathcal{G}}$ has zero mean and covariance matrix this identity matrix. Hence the clutter, conditioned on the variable S, is completely decorrelated through this linear transform.

We write this as $A\boldsymbol{\mathcal{G}} \stackrel{d}{=} CN(\mathbf{0}, I_{N \times N})$. Observe that $\boldsymbol{n}|S$ is still complex Gaussian with zero mean vector but covariance matrix $s^2 I_{N \times N}$, hence its density is

$$f_{\boldsymbol{n}|S=s}(\boldsymbol{x}) = \frac{1}{\pi^N s^{2N}} e^{-s^{-2}\|\boldsymbol{x}\|^2}, \tag{2.4}$$

where the norm in (2.4) is the complex Euclidean norm on vectors. Hence by using conditional probability [20]

$$f_{\boldsymbol{n}}(\boldsymbol{x}) \;=\; \int_0^\infty f_{\boldsymbol{n}|S=s}(\boldsymbol{x}) f_S(s) ds$$

$$\;=\; \int_0^\infty \frac{1}{\pi^N s^{2N}} e^{-s^{-2}\|\boldsymbol{x}\|^2} f_S(s) ds. \qquad (2.5)$$

Hence if we define a function $h_N(p)$ by

$$h_N(p) = \int_0^\infty s^{-2N} e^{-s^{-2}p} f_S(s) ds, \qquad (2.6)$$

then the clutter joint density can be written in the compact form

$$f_{\boldsymbol{n}}(\boldsymbol{x}) = \frac{1}{\pi^N} h_N(\|\boldsymbol{x}\|^2). \qquad (2.7)$$

The function h_N defined in (2.6) is of paramount importance in SIRP theory, as all densities of interest are expressed in terms of it. It is thus called the characteristic function. Much of the literature is devoted to determining h_N and f_S pairs for particular desired clutter models [6, 19].

Next we derive the marginal amplitude and intensity distributions of the complex clutter process $\boldsymbol{n}$, which are intimately related to the special function h_N. Let the kth element of $\boldsymbol{n}$ be n_k, so that $n_k = SA\boldsymbol{\mathcal{G}}_k$, where $\boldsymbol{\mathcal{G}}_k$ is the kth component of $\boldsymbol{\mathcal{G}}$, for $1 \le k \le N$. Then the complex Gaussian density of $A\boldsymbol{\mathcal{G}}_k$ is

$$f_{A\boldsymbol{\mathcal{G}}_k}(z) = \frac{1}{\pi} e^{-|z|^2}. \qquad (2.8)$$

Hence, equivalently, $A\boldsymbol{\mathcal{G}}_k$ is a complex Gaussian process with mean zero and covariance matrix $\frac{1}{2} I_{2\times 2}$. Consequently, it follows that its amplitude $|A\boldsymbol{\mathcal{G}}_k|$ has a Rayleigh distribution with parameter $\frac{1}{\sqrt{2}}$. Hence, using the fact that S and $A\boldsymbol{\mathcal{G}}_k$ are independent, and the definition of the Rayleigh density, we can show that

$$f_{|n_k|}(t) = \int_0^\infty \frac{2t}{s^2} e^{-\frac{t^2}{s^2}} f_S(s) ds = 2t h_1(t^2), \qquad (2.9)$$

yielding the marginal amplitude distribution for each k. Transforming to the intensity domain, it is not difficult to show

$$f_{|n_k|^2}(t) = \frac{1}{2} t^{-\frac{1}{2}} f_{|n_k|}(\sqrt{t}) = h_1(t), \qquad (2.10)$$

also for each k.

The importance of the results (2.9) and (2.10) is that they indicate how an arbitrary distribution can be embedded within a SIRP model. The key to the determination of a relevant SIRP for a given detection problem is the specification of the random variable S through its density f_S. For a desired marginal distribution, we can form an integral equation using (2.10) and (2.6) with $N = 1$. The literature contains extensive discussion of this problem; in particular, [6] contains guidelines on performing this, as well as case studies for most desired marginal distributions.

2.3 Pareto SIRP

The Pareto SIRP is defined to be that whose marginal intensity distributions are Pareto, with given parameters α and β. Recall that $X \overset{d}{=} Pa(\alpha, \beta)$ if its density is given by

$$f_X(t) = \begin{cases} 0 & t < \beta, \\ \frac{\alpha \beta^\alpha}{t^{\alpha+1}} & t \geq \beta. \end{cases} \tag{2.11}$$

The parameter α is called the distribution's shape parameter, while β is called the scale parameter. The latter specifies where on the real line the distribution's support begins, which is the interval $[\beta, \infty)$. The shape parameter controls how fast the distribution's tail decreases. In order to specify a multidimensional process of the form (2.1), we need to specify an appropriate density of S. The choice below has been based upon the results in [7].

Consider the function $f_S(s)$ defined by

$$f_S(s) = \frac{2\beta^\alpha}{\Gamma(\alpha)} s^{-2\alpha-1} e^{-\beta s^{-2}}, \tag{2.12}$$

for $s > 0$, where α and β are positive. An application of L'Hopital's Rule shows $\lim_{s \to o^+} f_S(s) = 0$, so we can set $f_S(0)$ equal to zero to make f_S continuous on the half interval $[0, \infty)$. Clearly $f_S(s) \geq 0 \ \forall s \geq 0$ and by a change of variables to $u = \beta s^{-2}$,

$$\int_0^\infty f_S(s) ds = \frac{\beta^{\alpha-1}}{\Gamma(\alpha)} \int_0^\infty \left(\frac{u}{\beta}\right)^{\alpha-1} e^{-u} du = 1, \tag{2.13}$$

using the definition of the Gamma Function. Hence the function $f_S(s)$ is a valid density on $[0, \infty)$.

It is not difficult to show that its first and second moments are given by

$$\mathbb{E}(S) = \frac{\sqrt{\beta}\Gamma(\alpha - 0.5)}{\Gamma(\alpha)} \text{ and } \mathbb{E}(S^2) = \frac{\beta}{\alpha - 1}. \tag{2.14}$$

Using this density, we determine the characteristic function h_N. By applying the transform $u = [p + \beta]s^{-2}$, we can show

$$
\begin{aligned}
h_N(p) &= \frac{2\beta^\alpha}{\Gamma(\alpha)} \int_0^\infty s^{-2N-2\alpha-1} e^{-[p+\beta]s^{-2}} ds \\[2mm]
&= \frac{\beta^\alpha}{\Gamma(\alpha)[p+\beta]^{N+\alpha}} \int_0^\infty u^{N+\alpha-1} e^{-u} du \\[2mm]
&= \frac{\beta^\alpha \Gamma(N+\alpha)}{\Gamma(\alpha)[p+\beta]^{N+\alpha}},
\end{aligned}
\tag{2.15}
$$

where the definition of the Gamma Function has been applied as previously.

Next we construct the marginal intensity distribution. By an application of (2.10), we see that by setting $N = 1$ in (2.15),

$$f_{|n_k|^2}(t) = \frac{\alpha\beta^\alpha}{[t+\beta]^{\alpha+1}}, \tag{2.16}$$

showing the marginal distributions corresponding to the whitened SIRP with the choice of $f_S(s)$ in (2.12) being shifted Pareto distributions. Note that the linear transform $z_k = |n_k|^2 + \beta$ yields a density

$$f_{z_k}(t) = f_{|n_k|^2}(t - \beta) = \frac{\alpha\beta^\alpha}{t^{\alpha+1}} \tag{2.17}$$

for $t \geq \beta$, which is the standard form of the Pareto density. Hence, the clutter process is modelled as a product of a random variable generated by S with density (2.12), and a complex Gaussian process with covariance matrix Σ. Note that since the Gaussian process is zero mean, $\mathbf{cov}(\boldsymbol{c}) = \mathbb{E}(S^2)\Sigma$, implying we can produce a desired covariance structure for our clutter process by scaling the Gaussian process by the mean squared value of S.

3   Neyman-Pearson Detectors

We now turn to the determination of optimal and suboptimal decision rules using the Neyman-Pearson Lemma [17] and the SIRP structure derived in the previous section. We begin with the case of a fully specified target model.

3.1   Case of a Completely Known Target

It is useful to begin with the case of a fixed known target model, which means we assume that R is a fixed constant that is completely specified.

Under H_1, $\boldsymbol{r} = R\boldsymbol{u} + \boldsymbol{n}$, and conditioned on S, this is still complex Gaussian, with the same covariance as $\boldsymbol{n}$ (since $R\boldsymbol{u}$ is constant), but its mean is shifted by the vector $R\boldsymbol{u}$. Hence the density under H_1 is

$$f_{H_1}(\boldsymbol{r}) = \frac{1}{\pi^N} h_N(\|\boldsymbol{r} - R\boldsymbol{u}\|^2). \tag{3.1}$$

Consequently, the Neyman-Pearson optimal detector is the ratio of the densities under H_1 and H_0. The density under H_0 is given by (2.7), with an application of (2.15). Hence the likelihood is

$$L(\boldsymbol{r}) = \frac{[\|\boldsymbol{r}\|^2 + \beta]^{N+\alpha}}{[\|\boldsymbol{r} - R\boldsymbol{u}\|^2 + \beta]^{N+\alpha}}, \tag{3.2}$$

using (3.1). Thus, the likelihood ratio test takes the form

$$M(\boldsymbol{r}) = \frac{\|\boldsymbol{r}\|^2 + \beta}{\|\boldsymbol{r} - R\boldsymbol{u}\|^2 + \beta} \underset{H_0}{\overset{H_1}{\gtrless}} \tau, \tag{3.3}$$

where τ is the detection threshold, which can be determined numerically from the false alarm specification. The notation $X \underset{H_0}{\overset{H_1}{\gtrless}} Y$ means that we reject H_0 if and only if $X > Y$. In all reasonable applications, we will not have knowledge of R, and so we must extend this result to account for an unknown R. This is the subject of the next subsection.

3.2   Unknown Target: Generalised Likelihood Ratio Test

In this case we assume R is unknown but constant within a given range profile. This means we can apply the GLRT to first estimate this parameter, and then apply the estimate to the test (3.3). The methodology of GLRT is described in [7, 10]. We essentially produce a suboptimal detector for the case of an unknown target, based upon the optimal decision rule formulated for a completely known target model.

We call this estimate $\hat{R}$, which is taken to be the maximum likelihood estimator [2]. It is chosen to minimise the quantity $\|\boldsymbol{r} - R\boldsymbol{u}\|^2$. This is because, in view of the density (3.1) and the definition of h_N in (2.6), maximising the density with respect to R is equivalent to minimisation of this quantity.

By applying a simple expansion, we can show

$$\|\boldsymbol{r} - R\boldsymbol{u}\|^2 = \|\boldsymbol{r}\|^2 + |R|^2\|\boldsymbol{u}\|^2 - 2\Re(R\boldsymbol{u}^H\boldsymbol{r}), \qquad (3.4)$$

where $\Re(z)$ is the real part of the complex number z. Recalling the proof of the Cauchy-Schwarz inequality (see [21] for example), this is minimised with the choice $\hat{R} = \frac{\boldsymbol{u}^H\boldsymbol{r}}{\|\boldsymbol{u}\|^2}$. Substituting this in (3.4) shows that

$$\min_R \|\boldsymbol{r} - R\boldsymbol{u}\|^2 = \|\boldsymbol{r} - \hat{R}\boldsymbol{u}\|^2 = \|\boldsymbol{r}\|^2 - \frac{|\boldsymbol{u}^H\boldsymbol{r}|^2}{\|\boldsymbol{u}\|^2}. \qquad (3.5)$$

An application of (3.5) to (3.3) results in the GLRT

$$L(\boldsymbol{r}) = \frac{\|\boldsymbol{r}\|^2 + \beta}{\|\boldsymbol{r}\|^2 - \frac{|\boldsymbol{u}^H\boldsymbol{r}|^2}{\|\boldsymbol{u}\|^2} + \beta} \underset{H_0}{\overset{H_1}{\gtrless}} \tau. \qquad (3.6)$$

This result is also derived in [7] in the context of sonar signal processing. However, our application is significantly different from that in the latter. The decision rule (3.6) gives a suboptimal detector for the detection of a target in clutter that has Pareto marginal distributions. The next Section will analyse its perfomance.

4   Detector Performance Analysis

The performance of the GLRT detector (3.6) is now examined. It will also be compared to the performance of the whitening matched filter (WMF), which can serve as a suboptimal decision rule. Determining when the WMF performs well is important because it does not depend on the clutter parameters, as does the GLRT solution. Four examples will be considered: the first two explore the role of the Pareto clutter parameters on detector performance. The second two examine the performance of the decision rules when applied to scenarios with Pareto parameters estimated from the 2004 Ingara data sets [22]. However, the clutter is simulated using the estimated parameters, to determine the receiver operating characteristic curves. Details of the Ingara clutter are not repeated here, but are available in a number of references. Refer to [3] and [22] for specific details of the data and trial, and [5] for information on the Pareto fit to the Ingara data.

For a given false alarm probability, the detection threshold τ has been estimated using Monte Carlo simulation. The number of independent and identically distributed samples

used is 10^6 in all cases. For a given SCR, the detection probability has also been estimated using Monte Carlo simulation, where for each given SCR, 10^6 independent and identically distributed samples have been used to estimate the detection probability.

4.1   Signal to Clutter Ratio

The signal to clutter ratio (SCR) measures the signal power relative to the clutter power. It is defined as $SCR = S_1/S_2$, where

$$S_1 = \mathbb{E}|R\boldsymbol{u}|^2 = \mathbb{E}[(R\boldsymbol{u})^H(R\boldsymbol{u})] = \mathbb{E}|R|^2\|\boldsymbol{u}\|^2. \tag{4.1}$$

Since R is assumed to be bivariate Gaussian, it follows that $|R|$ has a Rayleigh distribution with parameter σ, and so

$$\mathbb{E}|R|^2 = \mathbf{var}(|R|) + (\mathbb{E}(|R|))^2 = 2\sigma^2. \tag{4.2}$$

Next, the clutter has mean squared value

$$S_2 = \mathbb{E}|\boldsymbol{n}|^2 = \mathbb{E}(S^2)\mathbb{E}|A\boldsymbol{\mathcal{G}}|^2. \tag{4.3}$$

But recall the effect of the matrix A is that it decorrelates the Gaussian component $\boldsymbol{\mathcal{G}}$. Hence it is simple to show $\mathbb{E}|A\boldsymbol{\mathcal{G}}|^2 = N$, and so $S_2 = N\mathbb{E}(S^2)$. Consequently it follows that

$$SCR = \frac{2\sigma^2\|\boldsymbol{u}\|^2}{\mathbb{E}(S^2)N} = \frac{2\sigma^2\boldsymbol{p}^H\Sigma^{-1}\boldsymbol{p}}{\mathbb{E}(S^2)N} = \frac{2\sigma^2\boldsymbol{p}^H\Sigma^{-1}\boldsymbol{p}(\alpha-1)}{\beta N}, \tag{4.4}$$

using (2.14). In order to assess detector performance, the SCR is varied from -10 to +30 dB, and a Gaussian target model is used, whose parameters are determined from (4.4).

4.2   Whitening Matched Filter

As a comparison, the whitening matched filter, or Gaussian optimal detector is used as a suboptimal approximation. For a return $\boldsymbol{r}$, this decision rule takes the form

$$|\boldsymbol{u}^H\boldsymbol{r}|^2 \underset{H_0}{\overset{H_1}{\gtrless}} \tau_{wmf}, \tag{4.5}$$

where τ_{wmf} is the detector's threshold.

4.3   Receiver Operating Characteristics

A series of receiver operating characteristic (ROC) curves are now provided to assess detector performance. Throughout, a Toeplitz structure will be assumed for the clutter covariance matrix Σ. In particular, it will be assumed that $\Sigma(j,k) = \kappa^{|j-k|}$, for each $j, k \in \{0, 1, 2, \ldots N-1\}$, and $0 < \kappa < 1$. As pointed out in [3], the azimuth angle of Ingara is the angle the radar looks towards. For the Ingara trial, the wind speed is reported to have been 7.1 metres per second, in a direction of $47°$, for the Australian Government's Bureau of Meterology estimates. This means that the upwind angle is $227°$, which is the point where the clutter will be strongest [3].

All ROC curves show the performance of the suboptimal detectors relative to the optimal decision rule (3.3), denoted OPT throughout.

4.3.1   Example 1

The first set of ROC curves we examine explore the effect of the Pareto parameters on detector performance. Figure 4.1 is for the case where the number of looks is $N = 5$, the normalised Doppler frequency is $f_D = 0.5$, the probability of false alarm is 10^{-6} and the Toeplitz factor is $\kappa = 0.1$. The top two subplots in figure 4.1 show the effect of increasing the Pareto shape parameter α. The top left subplot is for the case where $\alpha = 3$ and $\beta = 1$. The top right subplot is for the case where $\alpha = 10$ and $\beta = 1$. These two plots show a phenomenon observed quite frequently in the ROC analysis. As the shape parameter is increased, the WMF becomes a good approximation to the GLRT detector. This is probably because the clutter is becoming more Gaussian like. The bottom two subplots in figure 4.1 show the effect of changing the scale parameter, while the shape parameter is held constant. The bottom left subplot is for $\alpha = 3$ and $\beta = 10$, while the bottom right subplot is for $\alpha = 3$ and $\beta = 100$. This was observed in other simulations: it appears that the scale parameter does not affect the detector's performance significantly. We observe that the GLRT has good performance throughout.

Figure 4.1: ROC curves. showing the effect of varying the Pareto parameters. Top left plot is for $\alpha = 3$ and $\beta = 1$, top right is for $\alpha = 10$ and $\beta = 1$. Bottom left is for $\alpha = 3$ and $\beta = 10$, bottom right is for $\alpha = 3$ and $\beta = 100$.
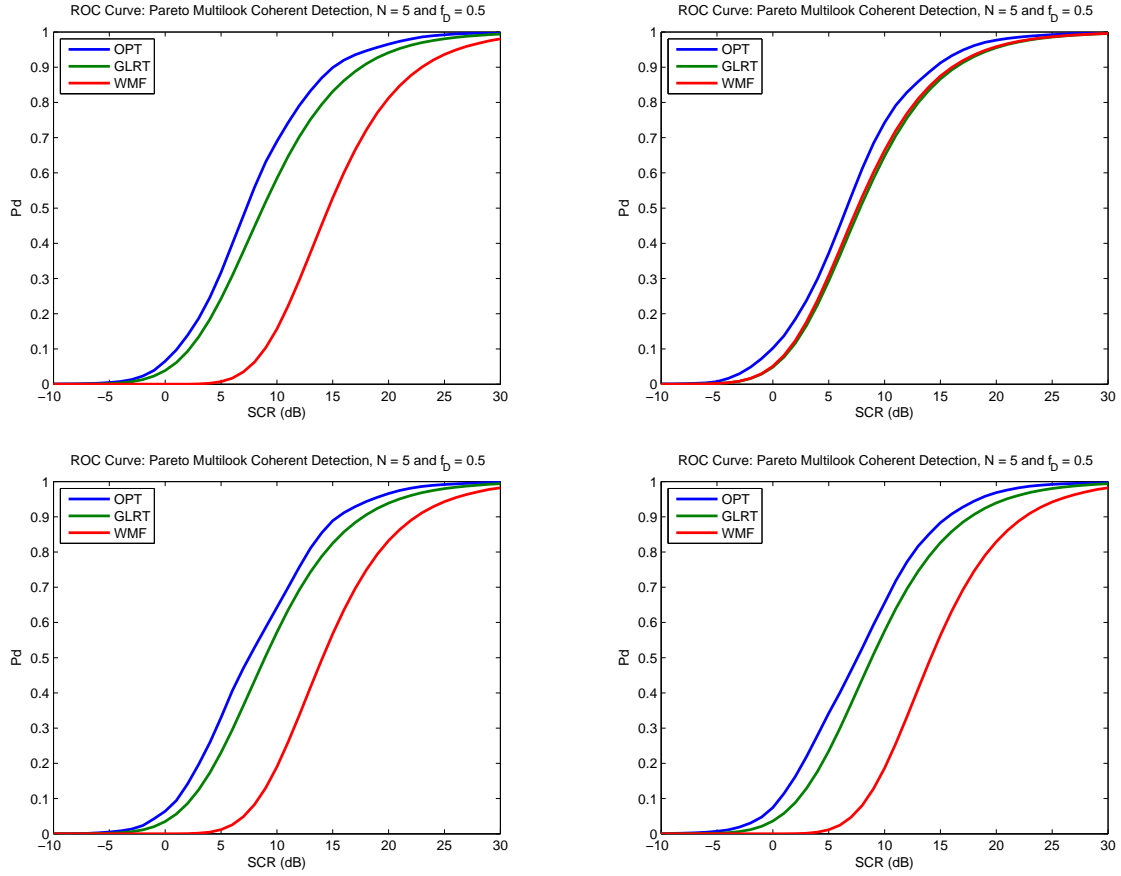

Figure 4.1: ROC curves. showing the effect of varying the Pareto parameters. Top left plot is for $\alpha = 3$ and $\beta = 1$, top right is for $\alpha = 10$ and $\beta = 1$. Bottom left is for $\alpha = 3$ and $\beta = 10$, bottom right is for $\alpha = 3$ and $\beta = 100$.

Figure 4.1: ROC curves. showing the effect of varying the Pareto parameters. Top left plot is for $\alpha = 3$ and $\beta = 1$, top right is for $\alpha = 10$ and $\beta = 1$. Bottom left is for $\alpha = 3$ and $\beta = 10$, bottom right is for $\alpha = 3$ and $\beta = 100$.

4.3.2   Example 2

As a second example, the effect of varying α, while the scale parameter is held fixed, is examined. Figure 4.2 is for the case where $N = 10$, $f_D = 1$, false alarm probability 10^{-6} and Toeplitz factor $\kappa = 0.9$ is considered. The scale parameter is fixed at $\beta = 0.01$, while the shape parameter is increased. This type of scale parameter has been found to be typical for horizontally polarised Ingara clutter returns, when modelled by a Pareto distribution. The top left plot in figure 4.2 is for $\alpha = 3$, the top right is for $\alpha = 10$, the bottom left is for $\alpha = 30$ and the bottom right subplot is for $\alpha = 50$. This example shows the WMF becoming a very good suboptimal decision rule as α increases. For large α, it matches the GLRT very closely. As before, the GLRT is always a good approximation to the optimal decision rule.

4.3.3   Example 3

The third example considered uses Pareto parameters estimated from the Ingara data sets. In this case, the parameters are sourced from run34683, at an azimuth angle of $225°$. This is only $2°$ off from the upwind direction, and so the clutter should be strong. Throughout, the normalised Doppler frequency has been set to $f_D = 0.4$, the Toeplitz factor $\kappa = 0.5$ and false alarm probability of 10^{-6}.

The top two subplots of figure 4.3 are for the vertically polarised case, where the Pareto parameters have been estimated to be $\alpha = 11.3930$ and $\beta = 0.3440$. The top left subplot has number of looks $N = 2$, while the top right is for $N = 8$. In this case, the WMF is a good approximation to the GLRT.

The bottom two subplots are for the horizontally polarised case, where the estimated Pareto parameters are $\alpha = 4.7241$ and $\beta = 0.0466$. The bottom left subplot is for $N = 2$ and the bottom right subplot is for $N = 8$. Here the WMF is not such a good approximation. In many of the Ingara data sets examined, this was found to be the case: the vertically polarised case resulted in the WMF being a good suboptimal detecor, while for horizontally polarised clutter, the GLRT is more suitable. The GLRT tends to only incur a small detection loss throughout.
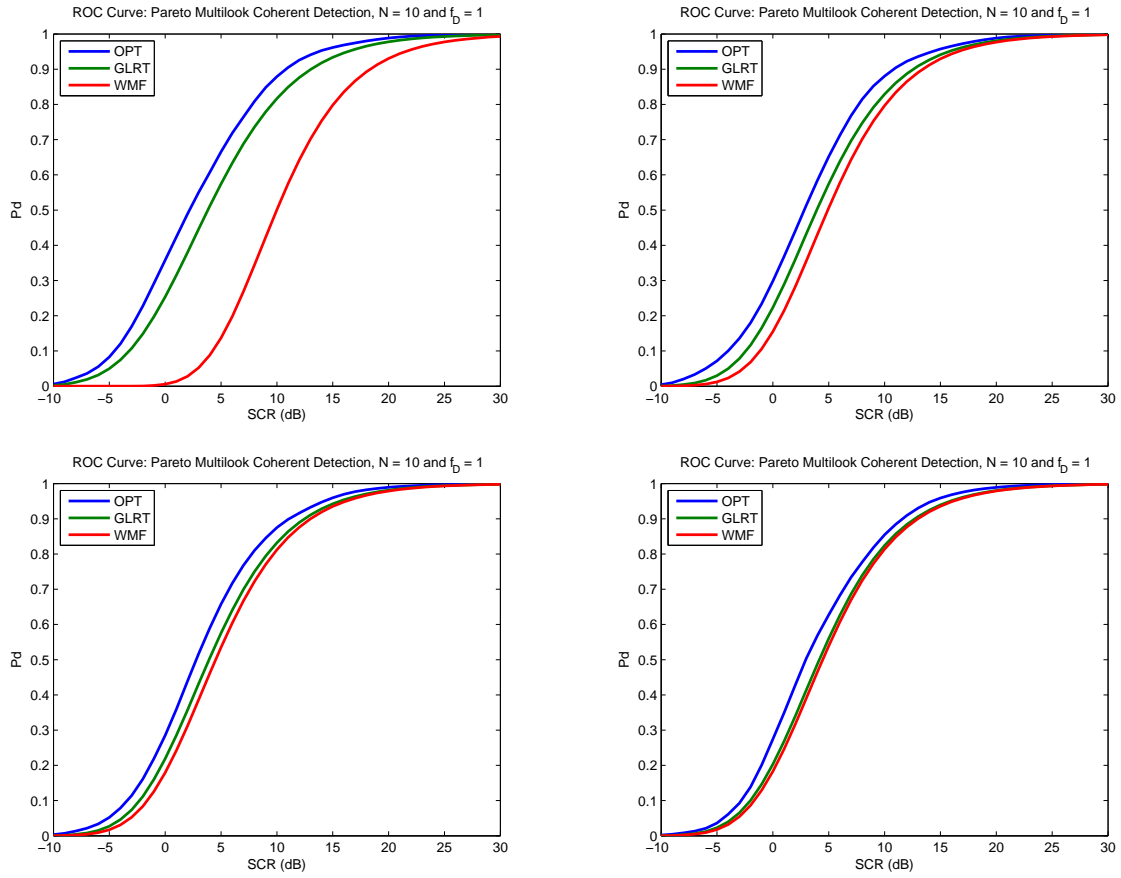
Figure 4.2: *ROC curves, showing the WMF becoming a better suboptimal decision rule as α is increased. In all cases, $\beta = 0.01$. Top left is for $\alpha = 3$, top right is for $\alpha = 10$, bottom left is for $\alpha = 30$ and bottom right is for $\alpha = 50$.*
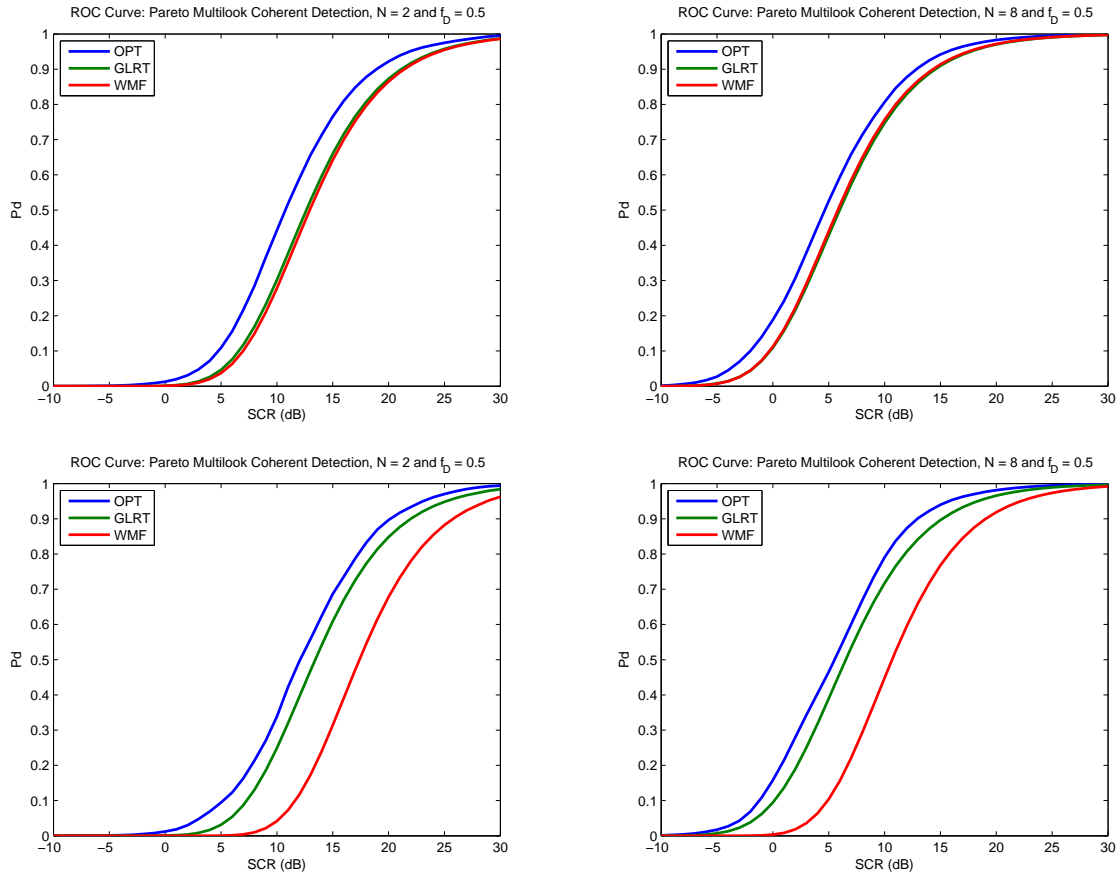
Figure 4.3: *ROC curves based upon the Ingara data set run34683. Top subplots are for vertical polarisation, bottom two are for horizontal polarisation. The WMF is suitable only for the vertically polarised case.*

4.3.4   Example 4

As a final example, the ROC performance of detectors with Pareto parameters sourced from run34683, at an azimuth of 190°, is considered. In this case, the clutter should be weaker because the radar is focused in the downwind direction (37° discrepancy from downwind). In this example, the normalised Doppler frequency has been set to $f_D = 0.5$, the Toeplitz factor is $\kappa = 0.01$ and false alarm probability of 10^{-6}. For the vertically polarised case, $\alpha = 8.9028$ and $\beta = 0.1109$. For the horizontally polarised case, $\alpha = 4.9031$ and $\beta = 0.0209$. Figure 4.4 shows the results. The top two plots are for the vertically polarised case, while the bottom two are for the horizontal polarisation. The number of looks is varied from $N = 2$ to $N = 8$, moving left to right as illustrated. For the vertically polarised case, we see that the WMF is a good approximation, while for the horizontally polarised case, it becomes better as the number of looks increases. Observe the GLRT has consistent performance.

4.4   Detector Computational Load Considerations

Due to the fact that a radar system must process many sets of returns rapidly, the relative computation loads of detectors is an important consideration in detector design. The WMF detector (equation 4.5) requires three operations (multiplication of Hermitian transpose vector and whitened return, followed by modulus and squaring). It is also independent of the clutter parameters. By contrast, the GLRT has a higher computational load (see equation 3.6). Given a whitened return $\boldsymbol{r}$, the GLRT involves calculation of the WMF, normalisation of it and then passing the result into a ratio function which requires computation of the modulus squared of the return $\boldsymbol{r}$. This can be done in a total of about 6 operations. However, these are not computationally intense operations[2]

As noted previously, the performance of the GLRT was matched by that of the WMF in a number of cases considered. Given this, the WMF could be used as a computationally cheaper solution.

---

[2]Examples of a high computational load is evaluation of Bessel functions and other integrals, such as is experienced with similar detectors for the case of K- and KK-Distributed clutter.
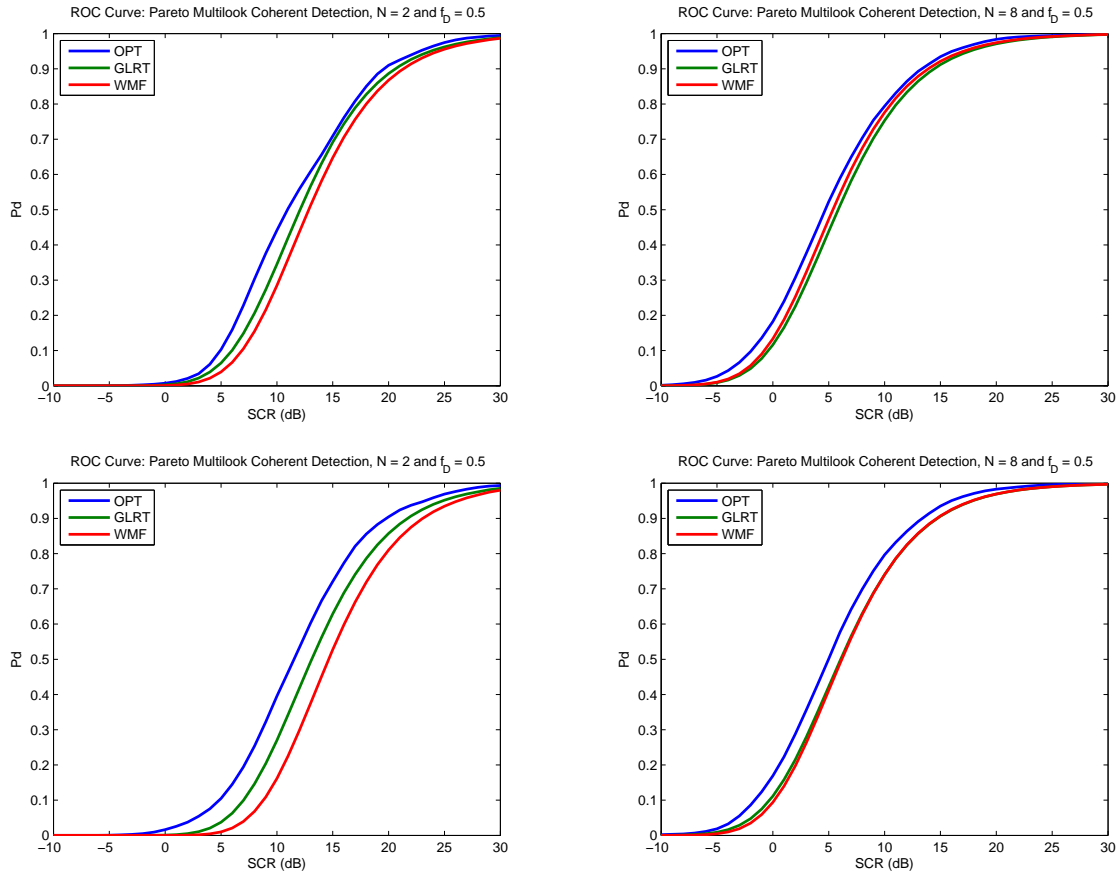
Figure 4.4: *ROC curves based upon Ingara data set run34683, with azimuth angle 190°. Top two subpolots are for the vertically polarised case, while bottom two are for horizional polarisation. For vertical polarisation, the WMF is a good approximation to the GLRT. For the horizontally polarised case, increasing the number of looks seems to make the WMF improve in performance.*

5 Conclusions

This report examined coherent multilook detection for targets in Pareto distributed clutter. By introducing the Pareto SIRP, the Neyman-Pearson Lemma yielded the theoretical optimal decision rule. From this, the suboptimal GLRT was constructed. It was shown to have small detection loss in a series of examples, some of which have been based upon Pareto clutter estimates sourced from Ingara data sets. The WMF was observed to be a good suboptimal approximation in a number of simulations, suggesting it can be used as a computationally simpler solution. The relationship between the WMF and GLRT will be explored in subsequent work, hopefully providing some general guidelines when the WMF is comparable to the GLRT. This will be advantageous from the perspective that it does not depend on the Pareto scale parameter, as does the GLRT.

6 Acknowledgements

References

1. Evans, M., Hastings, N. and Peacock, B., Statistical Distributions, 3rd Edition, (Wiley, New York, 2000).

2. Beaumont, G. P., 'Intermediate Mathematical Statistics', (Chapman and Hall, London, 1980).

3. Dong, Y., 'Distribution of X-Band High Resolution and High Grazing Angle Sea Clutter', (DSTO Report RR-0316, 2006).

4. Farshchian, M. and Posner, F. L., 'The Pareto Distribution for Low Grazing Angle and High Resolution X-Band Sea Clutter', IEEE Radar Conf., 789-793, 2010.

5. Weinberg, G. V., 'An Investigation of the Pareto Distribution as a Model for High Grazing Angle Clutter', DSTO Report TR-2525, 2011.

6. Rangaswamy, M, Weiner, D, and Ozturk, A, 'Non-Gaussian Random Vector Identification Using Spherically Invariant Random Processes', *IEEE Trans. Aero. Elec. Sys.* **29**, 111-123, 1993.

7. Barnard, T. J. and Khan, F., 'Statistical Normalization of Spherically Invariant Non-Gaussian Clutter', IEEE J. Ocean. Eng. **29**, 303-309, 2004.

8. Yao, K., 'A Representation Theorem and Its Application to Spherically-Invariant Random Processes', IEEE Trans. Info. Theory, **IT-19**, 600-608, 1973.

9. Wise, G. and Gallagher, N. C., On Spherically Invariant Random Processes, *IEEE Trans. Info. Theory* **IT-24**, 118-120, 1978.

10. Conte, E., Lops, M. and Ricci, G., 'Asymptotically Optimum Radar Detection in Compound Gaussian Clutter', *IEEE Trans. Aero. Elec. Sys.* **31**, 617-625, 1995.

11. Weinberg, G. V., 'Coherent Multilook Radar Detection for Targets in Pareto Distributed Clutter', *IET Elec. Letters* **47**, No. 14, 822-824, 2011.

12. Sangston, K. J., Gini, F. and Greco, M. S., 'New Results on Coherent Radar Target Detection in Heavy-Tailed Compound Gaussian Clutter', *IEEE Radar Conf.*, 779-784, 2010.

13. Piotrkowski, M., 'Distribution Independent CFAR Detector Using Extreme Value Theory', *Radar Symposium*, 2006.

14. Piotrkowski, M., 'Some Preliminary experiments with distribution-independent EVT-CFAR based on recorded radar data', *IEEE Radar Conf.*, 1-6, 2008

15. Shirman, Y. D. and Orlenko, V. M., 'Bayesian Theory of the Pareto Optimal CFAR Detectors', *Radar Symposium*, 2006.

16. Shang, X. and Song, H., 'Radar detection based on compound-Gaussian model with inverse gamma texture', *IET Radar, Sonar, Navig.* **5**, 315-321, 2011.

17. Neyman, J. and Pearson, E., On the Problem of the Most Efficient Tests of Statistical Hypotheses, *Phil. Trans. Royal Soc. Lond.* **Series A 231**, 289-337, 1933.

18. Conte, E. and Longo, M, Characterisation of radar clutter as a spherically invariant random process, *Proceed. IEEE***134 F**, 191-197, 1987.

19. Rangaswamy, M., Weiner, D. and Ozturk, A., Simulation of Correlated Non-Gaussian Interference for Radar Signal Detection, *Proceed. IEEE*, 148-152, 1991.

20. Durrett, R., Probability: Theory and Examples, 2nd Edition, (Wadsworth, California, 1996).

21. Kreyszig, E., Introductory Functional Analysis with Applications (Wiley, New York, 1978).

22. Crisp, D. J., Stacy, N. J. S. and Goh, A. S., 'Ingara medium-high incidence angle polarimetric sea clutter measurements and analysis', (DSTO Report TR-1818, 2006).

23. Gini, F., Greco, M. V., Farina, A. and Lombardo, P., Optimum and Mismatched Detection Against K-Distributed Plus Gaussian Clutter, *IEEE Trans. Areo. Elec. Sys.* **34**, 860-876, 1998.

DEFENCE SCIENCE AND TECHNOLOGY ORGANISATION DOCUMENT CONTROL DATA		1. CAVEAT/PRIVACY MARKING
2. TITLE Coherent Multilook Radar Detection for Targets in Pareto Distributed Clutter		3. SECURITY CLASSIFICATION Document (U) Title (U) Abstract (U)
4. AUTHOR Graham V. Weinberg		5. CORPORATE AUTHOR Defence Science and Technology Organisation PO Box 1500 Edinburgh, South Australia 5111, Australia

6a. DSTO NUMBER DSTO–TR–2646	6b. AR NUMBER AR-015-196	6c. TYPE OF REPORT Technical Report	7. DOCUMENT DATE January 2012

8. FILE NUMBER	9. TASK NUMBER AIR 07/040	10. TASK SPONSOR DGAD	11. No. OF PAGES 20	12. No. OF REFS 23

13. URL OF ELECTRONIC VERSION http://www.dsto.defence.gov.au/ publications/scientific.php	14. RELEASE AUTHORITY Chief, Electronic Warfare and Radar Division

15. SECONDARY RELEASE STATEMENT OF THIS DOCUMENT

Approved for Public Release

OVERSEAS ENQUIRIES OUTSIDE STATED LIMITATIONS SHOULD BE REFERRED THROUGH DOCUMENT EXCHANGE, PO BOX 1500, EDINBURGH, SOUTH AUSTRALIA 5111

16. DELIBERATE ANNOUNCEMENT

No Limitations

17. CITATION IN OTHER DOCUMENTS

No Limitations

18. DSTO RESEARCH LIBRARY THESAURUS

Target Acquisition	Maritime Detection
Maritime Surveillance	Sensors

19. ABSTRACT

The Pareto distribution has been proposed recently as a model for intensity clutter measurements, for maritime high resolution radar returns. Using the theory of spherically invariant random processes, the Neyman-Pearson optimal detector is derived. The generalised likelihood ratio test yields a simple suboptimal approximation, and its performance is gauged against the whitening matched filter.